MPPT algorithm for Voltage Controlled PV Inverters

T. Kerekes*, R. Teodorescu* , M. Liserre**, R. Mastromauro **, A. Dell'Aquila**

* Aalborg University/Institute of Energy Technology, Aalborg, Denmark
** Politecnico di Bari/ Dipartimento di Elettrotecnica ed Elettronica, Bari, Italy

***Abstract*—This paper presents a novel concept for an MPPT that can be used in case of a voltage controlled grid connected PV inverters. In case of single-phase systems, the 100Hz ripple in the AC power is also present on the DC side. Depending on the DC link capacitor, this power fluctuation can be used to track the MPP of the PV array, using the information that at MPP the power oscillations are very small. In this way the algorithm can detect the fact that the current working point is at the MPP, for the current atmospheric conditions.**

I. INTRODUCTION

Power supplied from a PV array depends mostly on present atmospheric conditions (irradiation and temperature), therefore in order to harvest the maximum available power the operating point needs to be tracked continuously using a Maximum Power Point Tracker (MPPT) algorithm [1][2][3][4]. Figure 1 presents the characteristic of a BPMSX120 PV panel, in case of standard test conditions (STC), which are: 25°C ambient temperature and 1000W/m^2 irradiation, highlighting the Maximum Power Point (MPP) at the top of the characteristic.

Most MPPT algorithms are based on the hill-climbing method and the MPP is found by changing the reference voltage of the PV, so that the extracted power is always the highest one for the present irradiation and temperature.

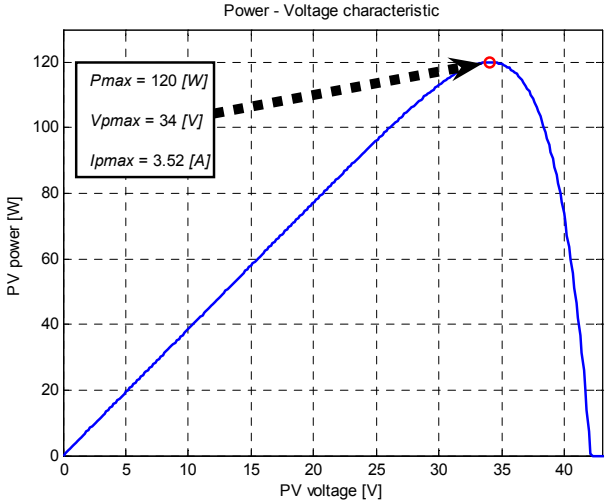

Figure 1. PV panel characteristic

In case of most single-stage grid connected PV systems, the control is acting on the grid side current only, which means that the MPPT is directly adjusting the amplitude of the grid current.

Now in case of a voltage control, the variable to adjust is the angle of the reference voltage, thereby ensuring the injection of only active power. When a distributed power generation system (DPGS) is connected to the grid, the grid frequency and the grid voltage can be controlled adjusting active and reactive power [5]. This can be done independently in case the line is mainly resistive (single-phase) or inductive (three-phase). In intermediate cases the control becomes more complex [6][7]. In this paper it will be assumed to have a mainly inductive grid.

II. VOLTAGE AND FREQUENCY SUPPORT

The power transfer from the DPGS to the grid, can be studied using short-line model and complex phasors, as shown in Figure 2, and the analysis is valid for both single-phase and balanced three-phase systems.

When the DG inverter is connected to the grid through a mainly inductive line X>>R, R may be neglected. If also the power angle δ is small, then $\sin\delta \cong \delta$ and $\cos\delta \cong 1$:

$$\delta \cong \frac{XP_A}{V_A V_B} \tag{1}$$

$$V_A - V_B \cong \frac{XQ_A}{V_A} \tag{2}$$

where V_A, P_A, Q_A denote respectively the voltage, the active power and the reactive power in section A and V_B is the voltage in section B, indicated in Figure 2.

For X>>R, a small power angle δ and a small difference $V_A - V_B$, equations (1) and (2) show that the power angle depends predominantly on the active power P, whereas the voltage difference $V_A - V_B$ depends predominantly on the reactive power Q. In other words the angle δ can be controlled regulating the active power P whereas the inverter voltage V_A is controllable through the reactive power Q. Control of the frequency

dynamically controls the power angle and, thus, the real power flow. Therefore by adjusting P and Q independently, frequency and amplitude of the grid voltage are determined.
These conclusions are the basis of the frequency and voltage droop controls through respectively active and reactive power [3].

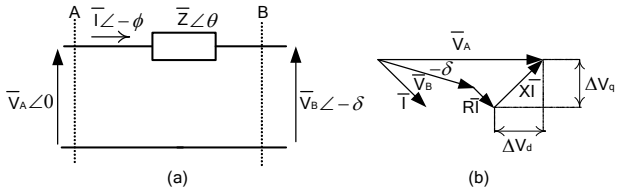

Figure 2. (a) Power flow through a line; (b) phasor diagram

III. CONVERTER VOLTAGE CONTROL

Commonly the shunt converter is current-controlled, but it is also possible to control the voltage directly in order to stabilize the voltage profile while the current injection is controlled indirectly as proposed in [8]. In this case the converter acts as a voltage source supplying the load and maintaining the load voltage constant and, at the same time, it compensates also the harmonics.

In this case the shunt converter is connected to the grid through an LCL filter as shown in Figure 5.

The adopted control method is based on a repetitive-based controller and it is shown in Figure 3. The voltage reference V_{ref} is given by the MPPT, so that the grid current I_g is synchronized to the grid voltage V_g.

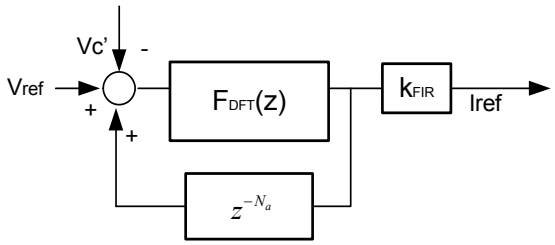

Figure 3. Repetitive-based controller

The repetitive controller ensures precise tracking of the selected harmonics and it provides the reference of the PI current controller, shown in Figure 4.

The repetitive controller is based on a finite-impulse response digital filter (FIR) [9] and it is defined as:

$$F_{DFT}(z)=\frac{2}{N}\sum_{i=0}^{N-1}\left(\sum_{k\in N_h}\cos\left[\frac{2\pi}{N}h\left(i+N_a\right)\right]\right)\cdot z^{-i} \quad (4)$$

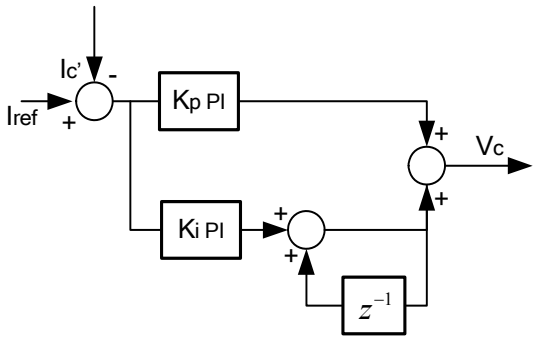

Figure 4. PI controller

where N_h is the set of selected harmonic frequencies, N_a is the number of leading steps determined by the stability analysis and N is the number of samples within one fundamental period. For the proposed system N=128 with a sampling frequency of 6400 Hz has been chosen. The parameters of the controller are reported in Table 1.

Table 1. Controller parameters

Controller Parameters of Shunt Converter	k_{FIR}	0.3
	N	128
	N_a	0
	$k_{p\text{-}PI}$	4.5
	$k_{i\text{-}PI}$	48

Controlling the voltage Vc', in presence of voltage variations, the grid current Ig is forced by the controller to have a sinusoidal waveform which is in phase with respect to the corresponding grid voltage [10].

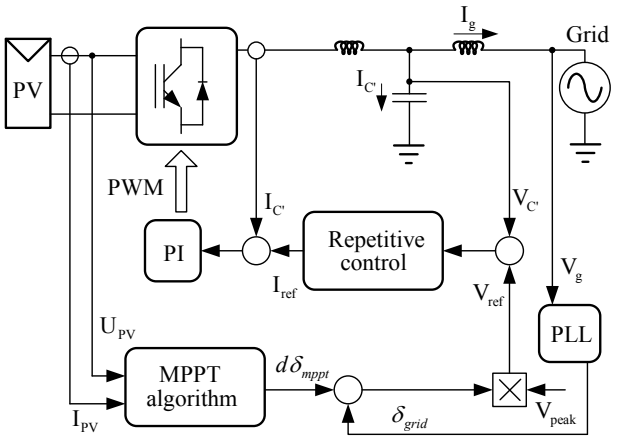

Figure 5. Voltage control of the PV converter

Figure 5 details the whole system, showing the hardware and the control algorithm, including all the feed-back from the plant.

IV. MPPT ALGORITHM

As mentioned before, in case of PV applications an MPPT algorithm is needed in order to be able to harvest the available maximum power that mainly depends on

solar irradiation and ambient temperature. The most widely used MPPT methods are the Perturb and Observe (P&O) and Incremental Conductance (INC). Both these methods are simple and easy to implement and their tracking efficiency is very high. From these two methods the INC method is able to tell whether the current working point is at the MPP of not, in case of ideal conditions. But due to noise in the measurements, the operating point could oscillate around the MPP.

In case of single phase systems, if a sweep is made over the whole PV characteristic, it can be observed, that within a period of 0.02s there are certain minimum and maximum values in the power and current oscillations, depending on the output power.

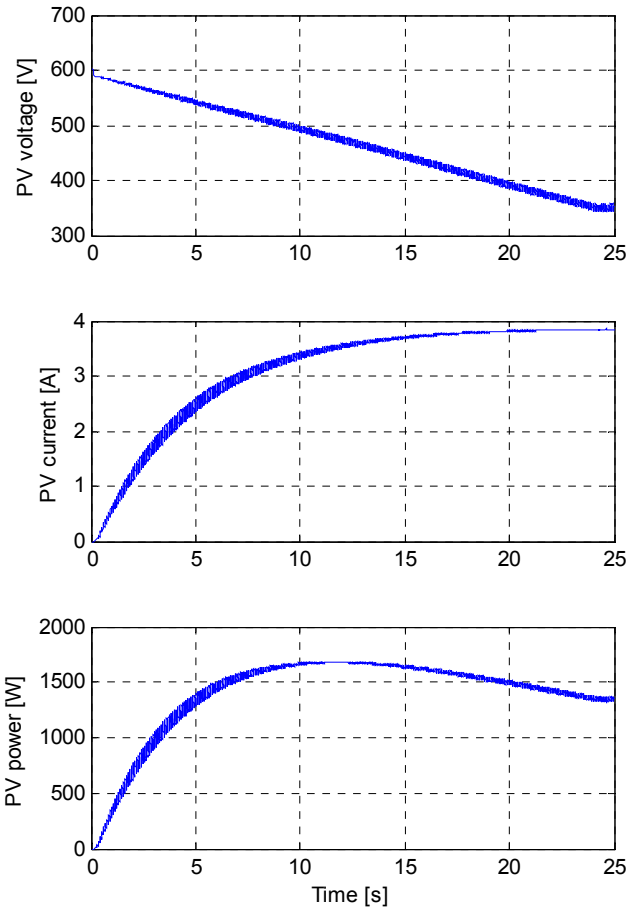

Figure 6. Power-sweep for the used PV array

As observed in Figure 6, the current oscillations are getting smaller the closer the PV current is to the short circuit current (I_{sc}). This is due to the fact that the PV behaves almost as a Voltage Source on the right side of the MPP and as a Current Source on the left side of the MPP as detailed in Figure 7.

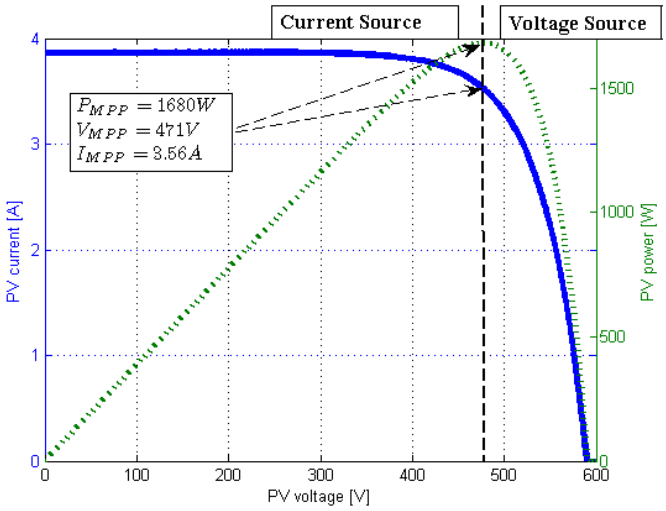

Figure 7. PV array characteristic

In order to clearly explain the basics of the idea, Figure 8, Figure 9 and Figure 10, present the three cases for the oscillations:

a) <u>Before the MPP</u>: when the PV panel behaves as a Voltage Source, the current oscillations are high, having values in the range of 0.2A, giving a power oscillation of 100W. It can also be observed that the power oscillations are in phase with the current oscillations, meaning that the current oscillations highly influence the power oscillations; (Figure 8)

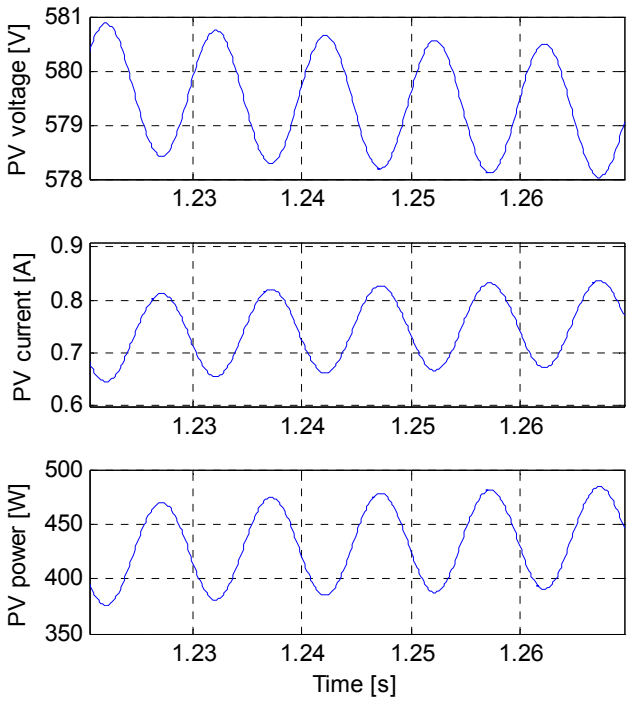

Figure 8. Oscillations before MPP (Voltage Source)

b) <u>At the MPP</u>: both current and voltage oscillations influence the power in the same way, therefore, the power oscillations are smaller (2W) and twice as fast (200Hz instead of 100Hz); (Figure 9)

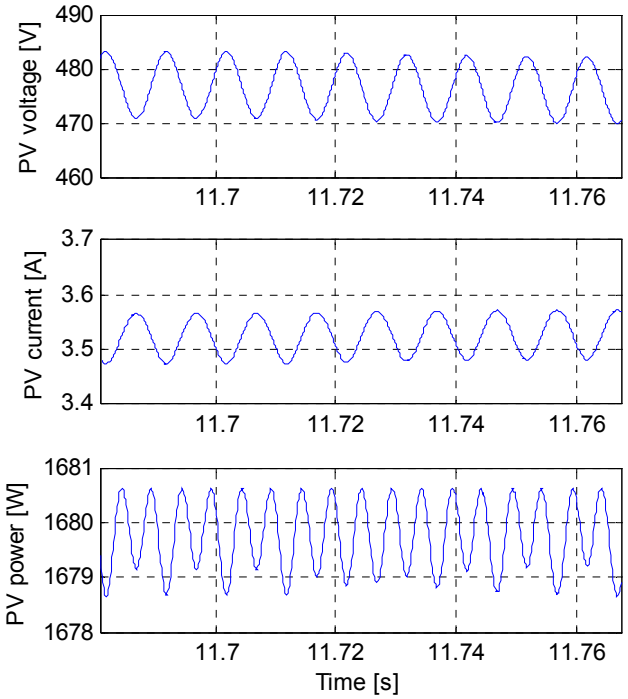

Figure 9. Oscillations at MPP

c) <u>After the MPP</u>: when the PV panel behaves as a Current Source, the current oscillations are very small, in the range of 0.01A. In this case the voltage oscillations influence the power oscillations, therefore the two oscillations are in phase; (Figure 10)

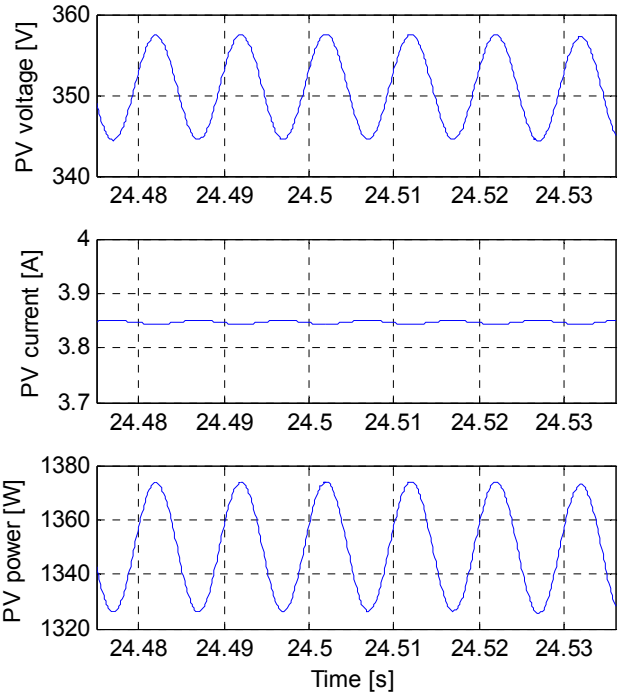

Figure 10. Oscillations after MPP (Current Source)

Now that the main idea of the algorithm has been introduced, the MPPT can be explained in detail.

The main feature that is added to the classical INC algorithm is the part which monitors the maximum and minimum values of the power oscillations on the PV side. Since this is a single-phase application, there is a 100Hz oscillation present in the output power, which is also present on the PV side. These minimum and maximum values of the PV power oscillation can be used to find out how close the current operating point is to the MPP, thereby slowing down the increment of the reference, in order not to cross the MPP.

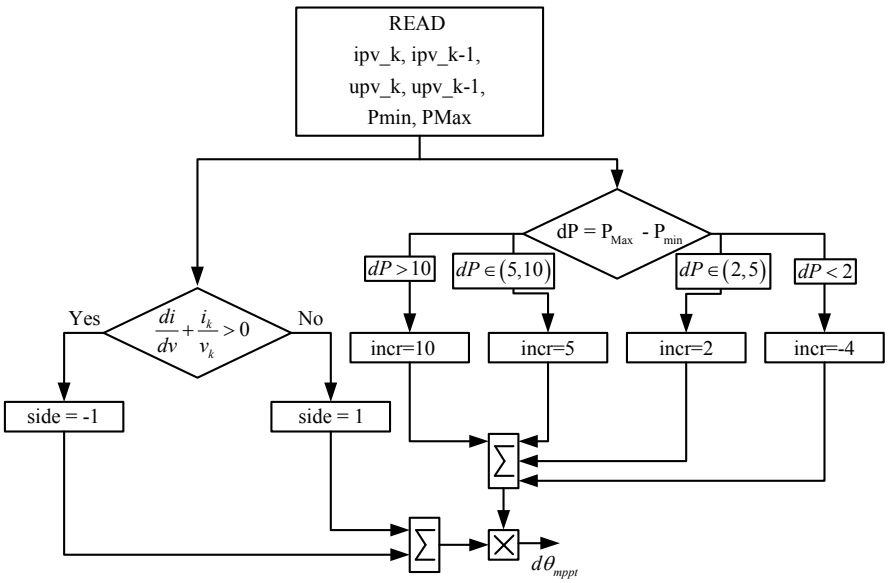

Figure 11. Flowchart of modified MPPT algorithm (dP-INC)

As explained before in Figure 8, Figure 9 and Figure 10, the power oscillation close to the MPP are very small, whereas far from the MPP there is a clear difference between the minimum and maximum values of the instantaneous PV power. Using this information, the proposed method (dP-INC) can detect that the current working point is close to the MPP or not and adjust the reference voltage of the voltage controller in order to harvest the available maximum power from the PV.

A flowchart of the dP-INC MPPT algorithm is shown on Figure 11, explaining how the angle of the reference voltage is modified, in order to track and keep the operating point as close to the MPP as possible.

For these simulations 14 series connected BP-MSX120 panels have been used, giving a maximum power of 1680W in case of STC. Figure 12 shows the hill-climbing of the MPPT algorithm for STC. The algorithm is triggered with 2Hz and the angle of the reference voltage is changed, as detailed in Figure 11. As seen in Figure 12, the power stabilizes at 1670W, which means that with this method the MPP (1680W) is reached with 99.48% efficiency, in case of the simulations with voltage control.

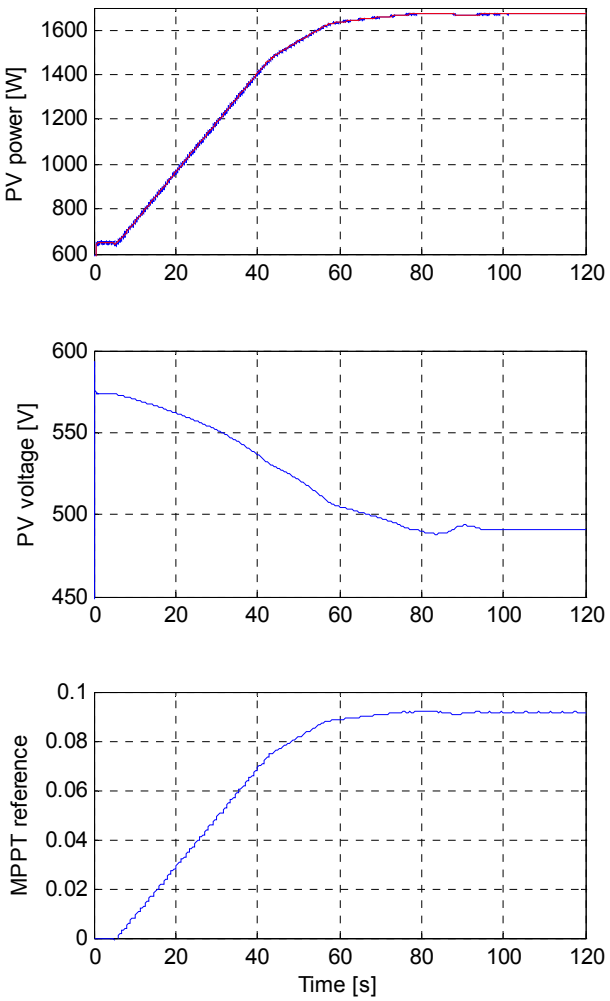

Figure 12. Hill-climb of MPPT algorithm

In order to show the performance of the proposed method the MPPT algorithm has also been tested in case of different irradiation conditions and compared with the classical P&O method. As seen in Figure 13 the irradiation has been changed according to the presented step function: 1000, 500, 300, 200, 100, 50, and back to 1000 W/m2 , each value being kept constant for 10 seconds in order to be sure that the MPPT algorithm has reached steady state conditions for each case. For these simulations the MPPT algorithm has been triggered every 0.1s. The efficiency of the MPPT is calculated using:

$$\eta_{MPPT} = \frac{P_{PV}}{P_{MPP}} \cdot 100 \qquad (3)$$

As seen on Figure 13 the algorithm can follow the MPP with a very high accuracy in case of high irradiation conditions. The efficiency is above 99.8%. The only case when the efficiency is lower than the previous limit is in case the irradiation was below 100W/m^2, in which case the efficiency was 99.6%, harvesting P_{PV}=130W instead of the ideal P_{MPP}=131W.

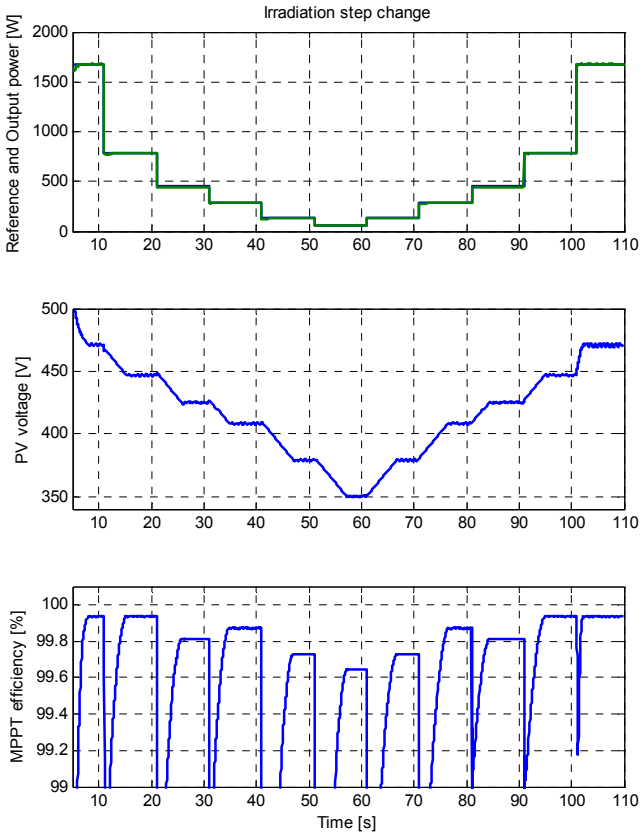

Figure 13. MPPT algorithm behavior in case of irradiation step change

The efficiency of the MPPT is calculated using:

$$\eta_{MPPT} = \frac{P_{PV}}{P_{MPP}} \cdot 100 \qquad (5)$$

As seen on Figure 13 the algorithm can follow the MPP with a very high accuracy in case of high irradiation conditions. The efficiency is above 99.8%. The only case when the efficiency is lower than the previous limit is in case the irradiation was below 100W/m^2, in which case

the efficiency was 99.6%, harvesting P_{PV}=130W instead of the ideal P_{MPP}=131W.

In order to have an idea about the performance of the proposed dP-INC MPPT algorithm, its performance has been compared with the classical P&O method. First a startup has been simulated, measuring the time needed for the hill-climb of both methods, in case of 1000W/m^2 irradiation. As detailed in Table 2, the P&O method needs 13s to arrive to the MPP, while the dP-INC gets there in a little bit more than 2s. The proposed method is faster because it uses bigger steps, when the working point is far from the MPP, therefore in certain cases arrives faster to the MPP, than the classical P&O.

In case of the irradiation step change, there has not been a big difference between the speeds of the two methods, as observed in the results detailed in Table 2.

V. CONCLUSIONS

A novel MPPT algorithm (dP-INC) has been presented, that can be used in case of voltage controlled PV inverters. As detailed the algorithm can detect whether the current working point is close to the MPP or not and adjust the increment accordingly. It can track the MPP with very high accuracy 99.9% in case of high levels of irradiation. The lowest efficiency of 99.6% was in case of 50W/m^2 irradiation.

Furthermore the algorithm has been compared with the classical P&O and the simulation results have shown that in certain cases the dP-INC method finds the MPP faster then the classical P&O, due to the fact that it uses bigger increments in case it is far from the MPP.

REFERENCES

[1] W. Xiao, J. Lind, W. Dunford, and A Capel, "Real-Time Identification of Optimal Operating Points in Photovoltaic Power Systems", IEEE Transactions on Industrial Electronics, vol.. 53, no. 4, August 2006.

[2] T. Esram, P.L.Chapman, Comparison of Photovoltaic Array Maximum Power Point Tracking Techniques IEEE Transactions on Energy Conversion, vol.. 22, no. 2, June 2007.

[3] J. Park, J. Ahn, B. Cho, and G. Yu, Dual-Module-Based Maximum Power Point Tracking Control of Photovoltaic Systems, Transactions on Industrial Electronics, vol.. 53, no. 4, August 2006.

[4] M. Calais, H. Hinz, "A Ripple-based Maximum Power Point Tracking Algorithm for Single-Phase, Grid Connected Photovoltaic System", Solar Energy Vol. 63, No. 5, pp. 277–282, 1998

[5] Josep M. Guerrero, José Matas, Luis García de Vicuña, Miguel Castilla, Jaume Miret, "Wireless-Control Strategy for Parallel Operation of Distributed-Generation Inverters", IEEE Transactions on Industrial Electronics , vol.53, no.5, Oct. 2006, pp. 1461-1470.

[6] Josep M. Guerrero, José Matas, Luis García de Vicuña, Miguel Castilla, Jaume Miret, "Decentralized Control for Parallel Operation of Distributed Generation Inverters Using Resistive Output Impedance", IEEE Transactions on Industrial Electronics , vol.54, no.2, April 2007, pp. 994-1004.

[7] K. De Brabandere, B. Bolsens, J. Van den Keybus, a. Woyte, J. Driesen, R. Belmans, "A Voltage and Frequency Droop Control Method for Parallel Inverters", IEEE Transactions on Power Electronics,vol.22, no.4,July 2007,pp.1107-1115.

[8] M. Routimo; M. Salo; H. Tuusa; "Current sensorless control of a voltage-source active power filter", Applied Power Electronics Conference and Exposition, 2005. APEC 2005. Twentieth Annual IEEE, Vol.3, Iss., 6-10, March 2005 pp. 1696- 1702.

[9] P. Mattavelli, F. Pinhabel Marafao, "Repetitive-Based Control for Selective Harmonic Compensation in Active Power Filter", IEEE Trans on Industrial Electronics, VOL.51 , NO.5, October 2004, pp. 1018-1024.

[10] R. Mastromauro; M. Liserre.; A. Dell'Aquila; "A grid-connected photovoltaic system with universal power quality conditioner functionality"; Proceedings of EPE 2007 – 12th European Conference on Power Electronics and Applications, 2-5 September 2007, Aalborg, Denmark.

Table 2: Performance comparison: P&O vs. dP-INC

W/m^2	Hill climb	1000→ 500	500→ 300	300→ 200	200→ 100	100→ 50	50→ 100	100→ 200	200→ 300	300→ 500	500→ 1000
P&O	13.1s	3s	2.5s	2s	3s	3s	3s	3s	2s	2.5s	3s
dP-INC	2.2s	2.5s	2.5s	2s	3s	3s	3s	3s	2s	2s	2s